

On the modelling of the point defects in the ordered B2 phase of the Ti-Al system

Wang, H.; Reed, R. C.; Gebelin, J. C.; Warnken, N.

DOI:

[10.1016/j.calphad.2012.06.007](https://doi.org/10.1016/j.calphad.2012.06.007)

License:

Creative Commons: Attribution (CC BY)

Document Version

Publisher's PDF, also known as Version of record

Citation for published version (Harvard):

Wang, H, Reed, RC, Gebelin, JC & Warnken, N 2012, 'On the modelling of the point defects in the ordered B2 phase of the Ti-Al system: Combining CALPHAD with first-principles calculations', *Calphad*, vol. 39, pp. 21-26. <https://doi.org/10.1016/j.calphad.2012.06.007>

[Link to publication on Research at Birmingham portal](#)

Publisher Rights Statement:

Elsevier Retrospective Gold article. This version is published in CALPHAD: Computer Coupling of Phase Diagrams and Thermochemistry [39(2012)21–26] DOI: <http://dx.doi.org/10.1016/j.calphad.2012.06.007>. This article is licensed under a CC-BY licence. The funders were work EPSRC (GrantNo.EP/F005946/1)

Eligibility for repository : checked 04/03/2014

General rights

Unless a licence is specified above, all rights (including copyright and moral rights) in this document are retained by the authors and/or the copyright holders. The express permission of the copyright holder must be obtained for any use of this material other than for purposes permitted by law.

- Users may freely distribute the URL that is used to identify this publication.
- Users may download and/or print one copy of the publication from the University of Birmingham research portal for the purpose of private study or non-commercial research.
- User may use extracts from the document in line with the concept of 'fair dealing' under the Copyright, Designs and Patents Act 1988 (?)
- Users may not further distribute the material nor use it for the purposes of commercial gain.

Where a licence is displayed above, please note the terms and conditions of the licence govern your use of this document.

When citing, please reference the published version.

Take down policy

While the University of Birmingham exercises care and attention in making items available there are rare occasions when an item has been uploaded in error or has been deemed to be commercially or otherwise sensitive.

If you believe that this is the case for this document, please contact UBIRA@lists.bham.ac.uk providing details and we will remove access to the work immediately and investigate.



On the modelling of the point defects in the ordered B2 phase of the Ti–Al system: Combining CALPHAD with first-principles calculations

H. Wang, R.C. Reed, J.-C. Gebelin, N. Warnken*

Department of Metallurgy and Materials, University of Birmingham, Edgbaston, Birmingham B15 2TT, UK

ARTICLE INFO

Article history:

Received 10 January 2012

Received in revised form

11 June 2012

Accepted 14 June 2012

Available online 25 July 2012

Keywords:

First-principles

CALPHAD

Point defects

B2

Ti–Al

ABSTRACT

First-principles calculations are performed in order to calculate the energies of formation of different point defects in the ordered B2 phase of the Ti–Al system. The dominant point defects in the sublattice of the B2–TiAl structure are determined to be either substitutional vacancies or anti-site defects. Based on the results of first-principles calculations, substitutional vacancies are considered in the sublattice for the CALPHAD assessment $(\text{Al,Ti,Va})_{0.5} : (\text{Al,Ti,Va})_{0.5}$. A self-consistent set of thermodynamic parameters is obtained. Phase equilibria in the Ti–Al binary system are reproduced using these thermodynamic parameters.

© 2012 Elsevier Ltd. All rights reserved.

1. Introduction

High strength β -Ti alloys were developed specifically for aerospace applications. The Boeing 777 aircraft for example was the first commercial airplane for which the volume of β alloys outnumbered the volume of Ti–6Al–4V [1]. The high strength of these alloys is affected by the α precipitation during the aging process, which is commonly related with the concentrations of thermal vacancies induced by the ordered structure—B2 [2,3]. The B2 structure has been found in many β alloy systems, such as Ti–25V–15Cr–6Al [4], Ti–Al–Nb [5], Ti–Al [6]. The present work treats the modelling of point defects (substitutional vacancy and anti-site defect) in the B2 structure of the Ti–Al system. First-principles calculations are used to study which are the predominant point defects, which then leads to a revised CALPHAD assessment of the B2 phase in the Ti–Al system.

2. Background

In recent thermodynamic descriptions of the Ti–Al binary system, the B2 phase is modelled using either a two-sublattice model $(\text{Al,Ti})_{0.5} : (\text{Al,Ti})_{0.5}$, or a three-sublattice one $((\text{Al,Ti})_{0.5} : (\text{Al,Ti})_{0.5} : \text{Va}_3$ which takes into account anti-site defects only [6–8]. This treatment differs from a previously proposed thermodynamic model

for the B2 phase $(\text{Al,Ni,Va})_{0.5} : (\text{Al,Ni,Va})_{0.5}$ in Ni–Al binary system, which considers both anti-site defects and substitutional vacancies [9]. Since the thermodynamic model of the B2 phase should reflect sound physical background, it is necessary to re-consider the model of the B2 phase on the basis of its known crystal structure.

Experimental studies of point defects in the B2 phase in the Ti–Al systems are hampered by the fact that bcc phase is not stable on the Al-rich side of the system. First-principles calculations are one way to overcome this limitation and to provide useful hints about the substitutional vacancy. Of course, results are limited, as calculation can only be done for the ground state. In order to overcome this limitation Hagen and Finnis [10] developed a method to study the point defects in the ordered alloys at finite temperatures which was then successfully applied to the B2 phase in the Ni–Al system. This method was used in the present work to calculate the concentration of different point defects located in different sites. The results of which were used to improve the thermodynamic model in the CALPHAD assessment of the Ti–Al binary system.

3. Methodology

3.1. First-principles calculations

The energies of various types of point defects were calculated by first-principles density functional theory, using a supercell approach which contains one defect (vacancy or antisite) in a large supercell (54-atom $3 \times 3 \times 3$). The all-electron Blöchl's

* Corresponding author. Tel.: +44 121 4143434.

E-mail address: n.warnken@bham.ac.uk (N. Warnken).

projector augmented wave approach [11,12] was used in the calculations within the generalized gradient approximation pot-paw_GGA, as implemented in the VASP software [13]. The Perdew–Burke–Ernzerhof (PBE) parameterisation [14,15] was used for the potpaw_GGA exchange–correlation functional. The valence configurations used for Ti are 4s3d, and those for Al are 3s3p. All the atoms were fully relaxed to the equilibrium positions. The other settings included plane-wave energy cutoff (450 eV), forces convergence cutoff (0.01 eV/Å) and Monk horst k-point meshes for Brillouin zone ($10 \times 10 \times 10$).

3.2. CALPHAD assessment

Ti-rich part of the Ti–Al phase diagram was re-optimised, while the Gibbs energies of all phases in the Al-rich part remained the same as the author's previous work [8]. Based on the results of the present work, the ordered bcc phase B2 and the corresponding disordered A2 phase are modelled as (Al,Ti,Va)_{0.5} : (Al,Ti,Va)_{0.5} and (Al,Ti,Va)₁, respectively. The hcp and Ti₃Al phases are modelled in accordance with the previous optimisation as (Al,Ti)₁ and (Al,Ti)_{0.75} : (Al,Ti)_{0.25}. Parameters were optimised using the Thermo-Calc software [16].

4. Results and discussion

4.1. The site preference of point defects

In order to calculate the energies of formation of different point defects, and thus to determine the thermodynamic model for the ordered B2 phase, the total energy E_{pure} of the perfectly stoichiometric TiAl was calculated first. After that the deviation from stoichiometry was taken into account by introducing four different point defects—one vacancy in Ti sublattice E_{VaTi} , one Al atom in Ti sublattice E_{AlTi} , one vacancy in Al site E_{VaAl} , and one Ti atom in Al site E_{TiAl} . All calculations were performed in the ground state, i.e., at zero temperature ($T=0$) and zero pressure ($p=0$). With these energies, it is still not possible to determine the preference of any sort of point defect, since it is not appropriate to simply compare the difference between the cases of substitutional vacancy and anti-site defect. In order to overcome this shortcoming, the enthalpies of formation of the point defects are calculated by using the rescaled total energies.

Define H_{i^k} (note: in this work the subscript i^k represents atom/vacancy $i=\text{Al, Ti, Va}$ in sublattice $k=\text{Al, Ti}$) as the enthalpy of formation of an alloy with respect to the energy of the standard states of the pure components (per atom) e_{TiTi} (hcp Ti) and e_{AlAl} (fcc Al)

$$H_{\text{VaAl}} = (E_{\text{VaAl}} - 27 \cdot e_{\text{TiTi}} - 26 \cdot e_{\text{AlAl}}) / 53 \quad (1)$$

$$H_{\text{TiAl}} = (E_{\text{TiAl}} - 28 \cdot e_{\text{TiTi}} - 26 \cdot e_{\text{AlAl}}) / 54 \quad (2)$$

$$H_{\text{VaTi}} = (E_{\text{VaTi}} - 26 \cdot e_{\text{TiTi}} - 27 \cdot e_{\text{AlAl}}) / 53 \quad (3)$$

$$H_{\text{AlTi}} = (E_{\text{AlTi}} - 26 \cdot e_{\text{TiTi}} - 28 \cdot e_{\text{AlAl}}) / 54 \quad (4)$$

$$H_{\text{pure}} = (E_{\text{pure}} - 27 \cdot e_{\text{TiTi}} - 27 \cdot e_{\text{AlAl}}) / 54 \quad (5)$$

For simplicity, the standard states of the two elements (fcc-Al and hcp-Ti) are used as reference states [17]. The calculated enthalpy of formation of the B2–TiAl is listed in Table 1 compared to various sources. Good agreement can be found between the present work and previous theoretical results. In Fig. 1, the calculated enthalpies of formation of the five blocks given above are plotted as four different branches. The point defects are sufficiently dilute in the calculations thus the enthalpies of formation of the alloys scale linearly with the atomic

Table 1

The calculated enthalpy of formation of the B2–TiAl compared to various sources; hcp Ti –7.8 eV/atom and fcc Al –3.7 eV/atom are used as reference state (Wan, 2004). Note the abbreviations are: PBE, Perdew–Burke–Ernzerhof parameterisation; GGA, generalised gradient approximation; EAM, embedded atom method; LAPW, linearised augmented planewave method; FLASTO, full-potential linearised augmented Slater-type orbital; LDA, local-density approximation; US-PP, ultrasoft pseudopotentials.

Values (kJ/mol)	Methods	Sources
–26.9	PBE/GGA	Present work
–26.1	EAM	[24]
–28.0	LAPW/GGA	[24]
–25.1	FLASTO/LDA	[25]
–25.9	US-PP/GGA	[19]
–39.4	CALPHAD	[26]
–37.2	CALPHAD	[6]

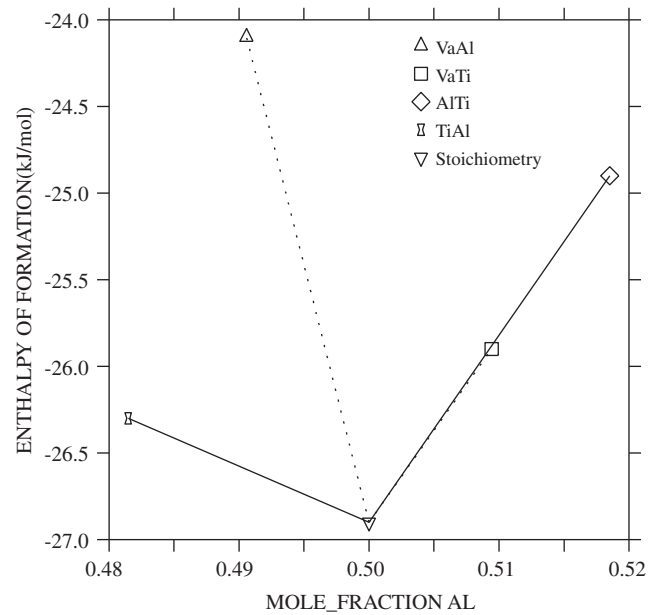


Fig. 1. The enthalpies of formation of five alloys.

concentrations of the point defects (note: the concentrations in the present work refer to concentrations per site, or site fraction). These four branches can be divided into two sets, one on each side of the perfect stoichiometric composition, corresponding to substitutional alloys containing anti-site defects and structural vacancies respectively. Point defects with lower enthalpy of formation are unambiguously more stable. Thus for Ti-rich alloys, the anti-site Ti defect is more stable than the vacancy, while in Al-rich alloy, the vacancy in the Ti sublattice is slightly more stable than the anti-site Al defect. This indicates that the preferred type of point defect is different on the Ti and Al side of the stoichiometric composition, with antisite atoms on the Ti side and vacancies Al on the Al rich side. This preference is confirmed by the calculation of point defect concentrations at finite temperature, as will be shown later. Some calculated enthalpies of formation are given in Table 2, such as those of isolated point defects (using Eqs. (6)–(9)), complex concentration-conserving defects and interbranch excitation

$$H_{\text{VaAl}}^F = 53 \cdot (H_{\text{VaAl}} - H_{\text{pure}}) \quad (6)$$

$$H_{\text{TiAl}}^F = 54 \cdot (H_{\text{TiAl}} - H_{\text{pure}}) \quad (7)$$

$$H_{\text{VaTi}}^F = 53 \cdot (H_{\text{VaTi}} - H_{\text{pure}}) \quad (8)$$

Table 2

The enthalpies of formation of isolated defects, complex concentration-conserving defects, and interbranch excitations in TiAl (hcp Ti -7.8 eV/atom and fcc Al -3.7 eV/atom are used as reference state (Wan, 2004)).

Name	Designation or quasichemical reaction	H_{ik}^F (eV)
Intrinsic point defects		
Ti in Al	Ti^{Al}	0.38
Vacancy in Al	Va^{Al}	1.54
Al in Ti	Al^{Ti}	1.15
Vacancy in Ti	Va^{Ti}	0.55
Concentration-conserving defect complexes		
Triple Ti (TT)	$0 \rightarrow 2Va^{Ti} + Ti^{Al}$	1.49
Divacancy (DV)	$0 \rightarrow Va^{Al} + Va^{Ti}$	2.10
Volume (E)	$0 \rightarrow Ti^{Al} + Al^{Ti}$	1.53
Triple Al (TA)	$0 \rightarrow 2Va^{Al} + Al^{Ti}$	4.23
Interbranch excitation		
Interbranch Ti	$Ti^{Al} \rightarrow 2Va^{Al}$	2.70
Interbranch Al	$2Va^{Ti} \rightarrow Al^{Ti}$	0.04

Table 3

The enthalpies of formation of the point defects (H_{ik}^F) based on different reference states: on the Ti-rich site, TiAl and Ti_3Al (-4.27 eV/atom for Al and -7.80 eV/atom for Ti); on the Al-rich site, TiAl and Ti_3Al_5 (-3.28 eV/atom for Al and -8.79 eV/atom for Ti) [19].

Name	Point defects	H_{ik}^F (eV)
Ti in Al	Ti^{Al}	-0.20
Vacancy in Al	Va^{Al}	1.26
Al in Ti	Al^{Ti}	-0.25
Vacancy in Ti	Va^{Ti}	-0.15
Interbranch Ti excitation	$Ti^{Al} \rightarrow 2Va^{Al}$	2.70
Interbranch Al excitation	$2Va^{Ti} \rightarrow Al^{Ti}$	0.04

$$H_{Al^{Ti}}^F = 54 \cdot (H_{Al^{Ti}} - H_{pure}) \quad (9)$$

It should be pointed out that an alternative way to subtract reference states is also presented as described by Zhang and Northrup [18]. On the Ti-rich site, the two defects Va^{Al} and Ti^{Al} are described with respect to TiAl and Ti_3Al : $e_{Ti^{Ti}} + e_{Al^{Al}} = E_{TiAl}$; $3 \times e_{Ti^{Ti}} + e_{Al^{Al}} = E_{Ti_3Al}$. On the Al-rich site, the other two defects Va^{Ti} and Al^{Ti} are referred to TiAl and Ti_5Al_3 : $e_{Ti^{Ti}} + e_{Al^{Al}} = E_{TiAl}$; $5 \times e_{Ti^{Ti}} + 3 \times e_{Al^{Al}} = E_{Ti_5Al_3}$ (note the total energies of the compounds are taken from Ghosh and Asta [19]). The calculated enthalpies of formation of the defects are listed in Table 3. It is found that the values of the enthalpies of formation of the defects are different, but the interbranch excitation of Ti and Al defects does not depend on the choice of the reference states, which has been mentioned in the work by Hagen and Finnis [10]. It is also noteworthy that since the enthalpy of formation of the interbranch Al defect is small (this enthalpy of formation is also affected by the calculation errors and atoms relaxations), a competition between triple and interbranch Al defects on the Al-rich side can be expected. Nevertheless, considering the present calculations, constitutional vacancies need be taken into account in the CALPHAD optimisations and this can be confirmed by predicting concentrations of the thermal defects which follows.

4.2. Vacancies at finite temperature

In this section, the concentration of substitutional vacancies at finite temperatures are evaluated. The concentrations of point defects are determined by using the results of first-principles calculations.

A linear relationship between the enthalpy of formation of an alloy H_k ($i = Al, Ti, Va$, $k = Al, Ti$) and the concentrations of the point defects x_k ($i = Al, Ti, Va$, $k = Al, Ti$) is given by

$$H_k = H_{pure} + \sum_i \sum_k H_{ik}^F x_{ik} \quad (10)$$

where H_{pure} corresponds to the enthalpy of formation of an alloy without point defects, and H_{ik}^F ($i = Al, Ti, Va$, $k = Al, Ti$) is the enthalpy of formation of one point defect, either anti-site defect or substitutional vacancy. In order to introduce temperature dependency, entropy needs to be taken into account; for the sake of simplicity only configurational entropy of the alloy is considered, such that

$$S = k \left((1 + x_{Va^{Al}} + x_{Va^{Ti}}) \ln \left(\frac{1 + x_{Va^{Al}} + x_{Va^{Ti}}}{2} \right) - \sum_i \sum_k x_{ik} \ln x_{ik} \right) \quad (11)$$

The equilibrium concentrations of the point defects are then calculated by combining minimisation of the Gibbs free energy ($G = H - TS = \min.$) with mass-balance constraints, consistent with

$$x_{Al^{Al}} + x_{Ti^{Al}} + x_{Va^{Al}} = 1 \quad (12)$$

$$x_{Ti^{Ti}} + x_{Al^{Ti}} + x_{Va^{Ti}} = 1 \quad (13)$$

$$x_{Al^{Al}} + x_{Al^{Ti}} = x_{Al} \quad (14)$$

$$x_{Ti^{Ti}} + x_{Ti^{Al}} = x_{Ti} \quad (15)$$

where x_{Al} and x_{Ti} are the total mole fraction of Al and Ti in the alloy, respectively. An analytical solution of this model, as derived in Refs. [10,20,21], is used in the present work. This yields the concentrations of point defects as functions of alloy composition and temperature.

The predicted concentrations of various point defects at $627^\circ C$ are plotted against the mole fraction of Al in Fig. 2. It becomes clear that substitutional vacancies are the major point defects on the Al-rich side. On the Ti-rich side the major point defects are anti-site Ti atoms, but the concentration of substitutional vacancies on the Ti sublattice is still relatively high. Higher concentrations of vacancies can be expected at higher temperatures than $627^\circ C$. The high concentration of substitutional vacancies is consistent with the experimental results, which indicates that ordering raises the vacancy concentration [2,3]. These results also illustrate the importance of including substitutional vacancies into the thermodynamic model for the B2 phase.

It is also interesting to separate structural from thermal point defects. Structural point defects are induced by the deviation from

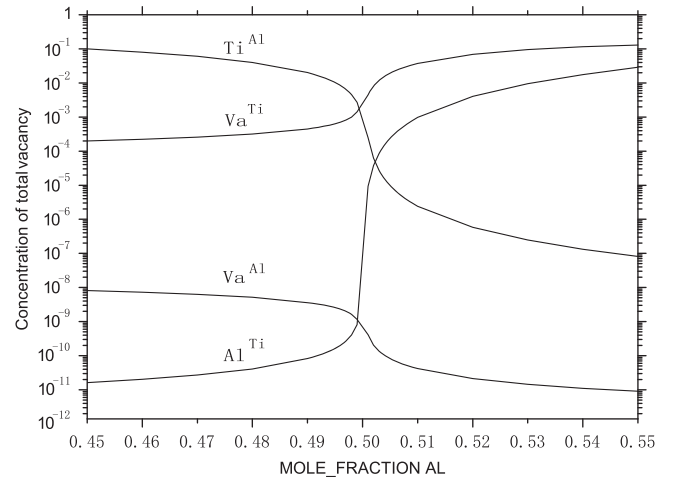


Fig. 2. The calculated concentrations of individual type of point defects at $627^\circ C$: Ti anti-site defect, Al anti-site defect, Ti vacancy and Al vacancy.

the exact stoichiometry. They are present at both 0 K and finite temperatures, while thermal point defects are present only at finite temperatures. In the following, only the major point defects obtained in Fig. 2 are considered (anti-site Ti defects on the Al sublattice and vacancies on the Ti sublattice). The concentrations of the thermal defects x_{ik}^t ($i = \text{Al, Ti, Va}$, $k = \text{Al, Ti}$) can be obtained as described by Lozovoi et al. [20]:

$$x_{ik}^t = x_{ik} - x_{ik}^0 \quad (16)$$

where x_{ik} and x_{ik}^0 ($i = \text{Al, Ti, Va}$, $k = \text{Al, Ti}$) are the concentrations of various types of point defects at finite temperature and 0 K, respectively. At 0 K two cases need be considered, depending on which is the dominant point defect on the sublattice under consideration:

(i) anti-site defect:

$$x_{ik}^0 = 2x_i - 1 \quad (17)$$

(ii) substitutional vacancy:

$$x_{ik}^0 = 1 - (1 - x_i)/x_i \quad (18)$$

in which x_i ($i = \text{Al, Ti}$) is the total mole fraction of i atoms in the i -rich alloy. The calculated concentrations of thermal defects are shown in Fig. 3. Interestingly vacancies on the Ti sublattice are the main point defects on the Ti-rich side, at an increasing concentration towards the stoichiometric composition, i.e. increasing Al alloy compositions. Similar behaviour is observed for anti-site Ti, but at lower defect concentrations. Above the stoichiometric composition ($> 50 \text{ at\% Al}$) the concentration of Ti vacancies steeply drops and thermal Ti vacancies are absent at any higher Al compositions. Similar behaviour is also found in the Ni–Al system, where it is attributed the interbranch Al excitation $2\text{VaTi} \rightarrow \text{AlTi}$ (see Table 2) [20]. Anti-site Al atoms are the dominant thermally induced point defects on the Al-rich side of the stoichiometry. Anti-site Ti is predicted at similar concentration close to the stoichiometric composition, but quickly drops to much lower values at higher Al alloy compositions.

4.3. Phase diagram

The thermodynamic description of the Ti–Al binary system was revised, based on the information on point defects presented in this work. The revised description is largely based on a

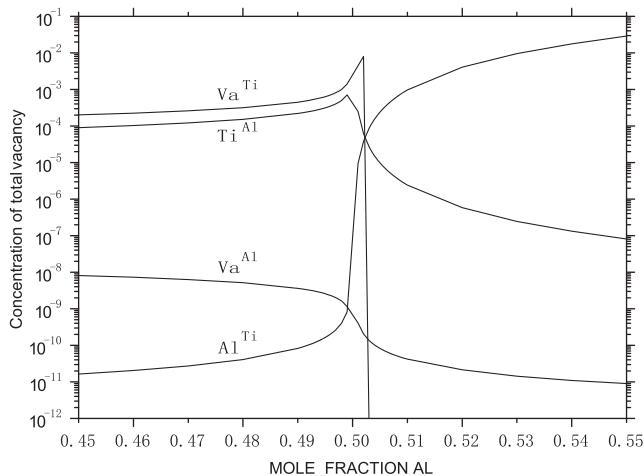


Fig. 3. The calculated concentrations of thermal defects at 627 °C: Ti anti-site defect, Al anti-site defect, Ti vacancy and Al vacancy.

previously published assessment [22]. In order to reflect the influence of point defects, substitutional vacancies were added into the thermodynamic model of the ordered B2 phase— $(\text{Al, Ti, Va})_{0.5} : (\text{Al, Ti, Va})_{0.5}$, and the model for the corresponding disordered A2 phase therefore becomes $(\text{Al, Ti, Va})_1$. These changes also affect the parameters of the α and α_2 phases, the revised parameters of these are given in Table 4 and the corresponding phase diagram is shown in Fig. 4. Furthermore, Table 5 shows the temperatures and compositions of the two relevant peritectoid reactions in comparison to those found in other sources. Besides a sounder physical description, a better consistency with experimental data of phase equilibria is observed.

Fig. 5 shows the calculated Ti–Al phase diagram without the ordered B2 phase. In this case the bcc-hcp does not show the peculiar bending as seen in Fig. 4, and the α_2 phase (Ti_3Al) forms congruently from the α (hcp) phase at 1164 °C. The same diagram, calculated using the author's previous description is also shown, using dotted lines [8]. It can be seen that the temperature of congruent formation of α_2 has increased after the re-optimisation. Taking the B2 phase into account will cause the bcc-hcp two phase region to bend sufficiently to form the $\beta + \alpha \rightarrow \alpha_2$ peritectoid reaction. However, the maximum temperature of this reaction cannot be higher than the temperature of congruent formation of α_2 . The introduction of point defects into the A2/B2 model and the re-optimisation of the Ti rich part of the phase diagram did increase the temperature of congruent α_2 formation sufficiently, to raise the temperature of the peritectoid reaction from 1160 °C to 1198 °C. This is in very good agreement with the most recent assessment of the Ti–Al phase diagram by Schuster and Palm [23].

Fig. 6 shows the vacancy concentration in the B2 phase versus temperature as obtained from CALPHAD calculations for Ti–30 at% Al. This alloy shows a B2 single phase region between 1210 °C and 1490 °C. An increase of the vacancy concentration with temperature is found up to about 1200 °C followed by a

Table 4

Thermodynamic parameters of the phases in the Ti-rich part of Ti–Al binary system (note that the parameters of the A2 phase are originally from [27], and the Gibbs energy functions GALHCP, GHSERAL and GHSERTI are from [28]).

Thermodynamic parameters	Value (J/mol)
G(BCC_A2,AL,TI;0)	− 121 785 + 34.0*T
G(BCC_A2,AL,VA;0)	60 000
G(BCC_A2,TI,VA;0)	150 000
G(BCC_B2,AL;0)	0
G(BCC_B2,TI;0)	− 21 645 + 3.1*T
G(BCC_B2,VA;0)	5000 − 0.5*T
G(BCC_B2,AL;TI;0)	− 21 645 + 3.1*T
G(BCC_B2,TI;TI;0)	0
G(BCC_B2,VA;TI;0)	26 645 − 3.6*T
G(BCC_B2,AL;VA;0)	5000 − 0.5*T
G(BCC_B2,TI;VA;0)	26 645 − 3.1*T
G(BCC_B2,VA;VA;0)	0
G(BCC_B2,AL;TI,VA;0)	− 75 000
G(BCC_B2,TI,VA;AL;0)	− 75 000
G(BCC_B2,TI,AL;TI;0)	− 7080
G(BCC_B2,AL,TI;TI;0)	− 7080
G(BCC_B2,TI;AL,TI;1)	− 3150
G(BCC_B2,AL;TI;TI;1)	− 3150
G(HCP_A3,AL,TI,VA;0)	− 128 189 + 35.2*T
G(HCP_A3,AL,TI,VA;1)	16 034.9 − 12.2*T
G(TI3AL,AL;AL;0)	GALHCP
G(TI3AL,AL;TI;0)	32 363.6 − 8.25*T + 0.75*GHSERAL + 0.25*GHSERTI
G(TI3AL,TI;AL;0)	− 32 363.6 + 8.25*T + 0.75 *GHSERTI + 0.25*GHSERAL
G(TI3AL,TI;TI;0)	GHSERTI
G(TI3AL,AL,TI;AL;0)	− 71 277.9 + 25.5*T
G(TI3AL,AL,TI;TI;0)	− 71 277.9 + 25.47*T

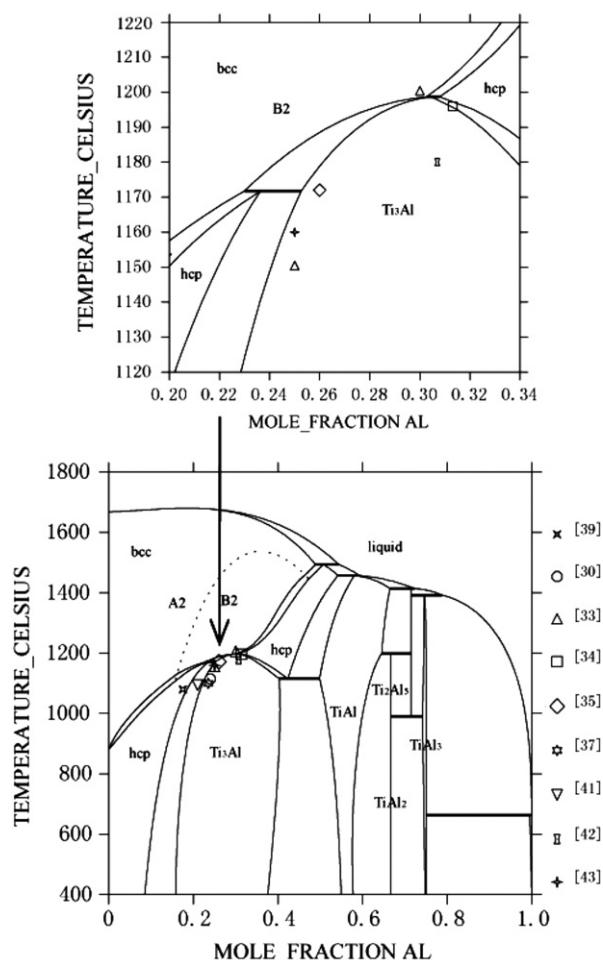


Fig. 4. The calculated Ti-Al binary phase diagram versus experimental data.

Table 5

Calculated results of the invariant reactions involving the B2 phase in the Ti-Al binary system compared with experimental or assessed phase equilibria.

Invariant reaction	T (°C)	x(Al) (at%)			Ref.
		β	α	α_2	
$\beta + \alpha \rightarrow \alpha_2$	≈ 1250	–	–	–	[29]
	1215	–	–	–	[30]
	≈ 1150	–	–	–	[31]
	≈ 1135	–	–	–	[32]
	≈ 1200	≈ 29	35	30	[33]
	1196	28.7	32	31.3	[34]
	1200 ± 10	≈ 28	33	32	[23]
	1162	31.3	32.4	32	[8]
	1198	30.2	30.8	30.5	This work
		β	α_2	α	
$\beta + \alpha_2 \rightarrow \alpha$	1172 ± 8	23.9	28	26	[35–37]
	1100	15.5	25.3	23.5	[38]
	1080 ± 20	15	22.5	17.5	[29,39]
	1100	15.7	25.3	21	[40,41]
	1180	18.7	26	≈ 30.7	[42]
	1115	16	27	24	[30]
	≈ 1150	24	26	25	[33]
	1160 ± 10	21.5	26	25	[43]
	1170 ± 10	25	27.5	27	[23]
	1124	24.7	26.8	26	[8]
	1172	23.0	25.3	23.6	This work

decrease at higher temperatures. This is consistent with creation of vacancies due to increase of temperature, and their loss due to reduced degrees of ordering, which reflects greater opportunity of

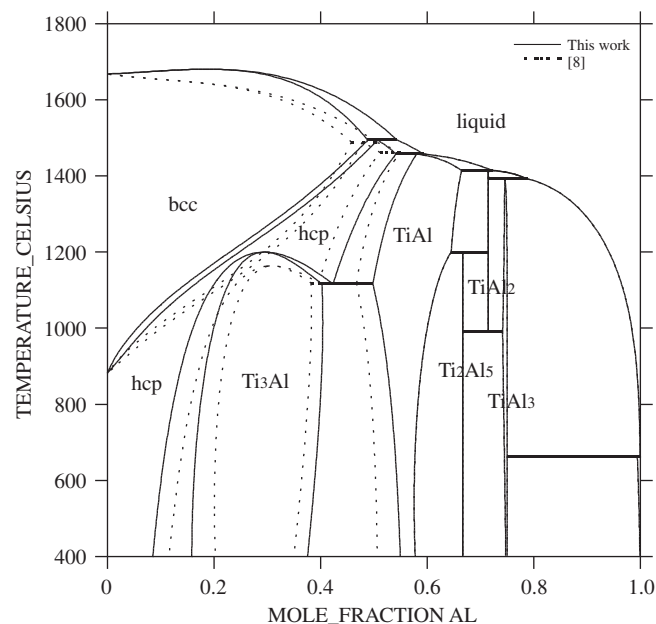


Fig. 5. The comparison between the phase diagrams without the B2 phase.

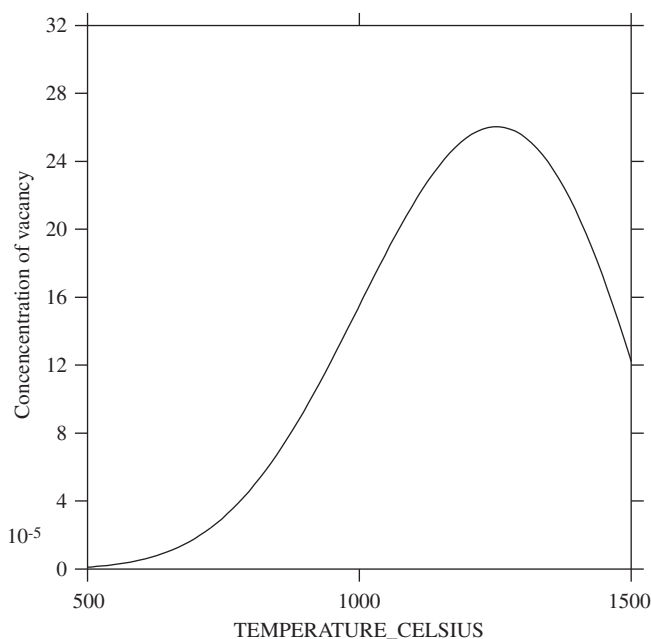


Fig. 6. The concentration of vacancy in the B2 phase (Ti-30 at% Al, stable between 1210 and 1490 °C from CALPHAD results) versus temperature.

random arrangement of atoms in the crystal lattice. Calculations of vacancy concentrations using CALPHAD can be very helpful to explain vacancy related effects at high temperatures – such as rapid precipitate growth in quenched alloys – especially when extrapolated to more complex alloys.

5. Conclusions

The enthalpies of formation of different point defects in the B2 phase of the Ti-Al system are calculated using first-principles calculations. The preference of the point defects is predicted—Ti anti-site defect in the Al sublattice and vacancy in the Ti sublattice. The concentrations of various types of point defects were calculated at finite temperatures using first-principles

calculations. Substitutional vacancies were added into the thermodynamic model of the B2 phase, which is now modelled as $(\text{Al,Ti,Va})_{0.5} : (\text{Al,Ti,Va})_{0.5}$. The Ti–Al binary system was re-optimised, which resulted in a better reproduction of experimental phase equilibria.

Acknowledgements

This work is financially supported by EPSRC (Grant No. EP/F005946/1). Thanks are given to Prof. X. Wu, Prof. M. Loretto, Dr. A. Mottura and Dr. X.M. Tao during the course of this work.

Appendix. Supporting information

Supplementary data associated with this article can be found in the online version at <http://dx.doi.org/10.1016/j.calphad.2012.06.007>.

References

- [1] G. Lutjering, J.C. Williams, *Titanium*, Springer, 2003.
- [2] P.R. Munroe, The effect of nickel on vacancy hardening in iron-rich FeAl, *Intermetallics* 4 (1996) 5.
- [3] M.A. Morris, O. George, D. Morris, Vacancies, vacancy aggregates and hardening in FeAl, *Mater. Sci. Eng. A* 258 (1998) 99.
- [4] Y.G. Li, P.A. Blenkinsop, M.H. Loretto, N.A. Walker, Effect of aluminium on ordering of highly stabilised β -Ti–V–Cr alloys, *Mater. Sci. Technol.* 14 (1998) 732.
- [5] K. Das, S. Das, Order-disorder transformation of the body centered cubic phase in the Ti–Al–X (X=Ta, Nb, or Mo) system, *J. Mater. Sci.* 38 (2003) 3995.
- [6] I. Ohnuma, Y. Fujita, H. Mitsui, K. Ishikawa, R. Kainuma, K. Ishida, Phase equilibria in the Ti–Al binary system, *Acta Mater.* 48 (2000) 3113.
- [7] V.T. Witusiewicz, A.A. Bondar, U. Hecht, S. Rex, T.Y. Velikanova, The Al–B–Nb–Ti system. III. Thermodynamic re-evaluation of the constituent binary system Al–Ti, *J. Alloys Compd.* 465 (2008) 64.
- [8] H. Wang, N. Warnken, R.C. Reed, Thermodynamic and kinetic modeling of bcc phase in the Ti–Al–V ternary system, *Mater. Sci. Eng. A* 528 (2010) 622.
- [9] N. Dupin, I. Ansara, On the sublattice formalism applied to the B2 phase, *Z. Metallk.* 90 (1999) 76.
- [10] M. Hagen, M.W. Finnis, Point defects and chemical potentials in ordered alloys, *Philos. Mag.* A 77 (1998) 447.
- [11] P.E. Blöchl, Projector augmented-wave method, *Phys. Rev. B* 50 (1994) 17953.
- [12] G. Kresse, D. Joubert, From ultrasoft pseudopotentials to the projector augmented-wave method, *Phys. Rev. B* 59 (1999) 1758.
- [13] J. Hafner, Ab-initio simulations of materials using vasp: density-functional theory and beyond, *J. Comput. Chem.* 29 (2008) 82.
- [14] J.P. Perdew, K. Burke, M. Ernzerhof, Generalized gradient approximation made simple, *Phys. Rev. Lett.* 77 (1996) 3865.
- [15] J.P. Perdew, K. Burke, M. Ernzerhof, Erratum: generalized gradient approximation made simple, *Phys. Rev. Lett.* 78 (1997) 1396.
- [16] J.O. Andersson, T. Helander, L. Höglund, P.F. Shi, B. Sundman, Thermo-calc & Dictra, computational tools for materials science, *Calphad* 26 (2002) 273.
- [17] Y. Wang, S. Curtarolo, C. Jiang, R. Arroyave, T. Wang, G. Ceder, L.-Q. Chen, Z.-K. Liu, Ab initio lattice stability in comparison with CALPHAD lattice stability, *Calphad*, 28 (1) (2004) 79.
- [18] S.B. Zhang, John E. Northrup, Chemical potential dependence of defect formation energies in GaAs: application to Ga self-diffusion, *Phys. Rev. Lett.* 67 (1991) 2339.
- [19] G. Ghosh, M. Asta, First-principles calculation of structural energetics of Al–TM (TM=Ti, Zr, Hf) intermetallics, *Acta Mater.* 53 (2005) 3225.
- [20] A. Lozovoi, K. Ponomarev, Yu. Vekilov, P. Korzhavyi, I. Abrikosov, First-principles investigation of thermal point defects in B2 NiAl, *Phys. Solid State* 41 (1999) 1494.
- [21] C. Jiang, D.J. Sordelet, B. Gleeson, Site preference of ternary alloying elements in Ni₃Al: a first-principles study, *Acta Mater.* 54 (2006) 1147.
- [22] F. Zhang, F.-X. Xie, S.-L. Chen, Y.A. Chang, D. Furrer, V. Venkatesh, Predictions of titanium alloy properties using thermodynamic modeling tools, *J. Mater. Eng. Perform.* 14 (2005) 717.
- [23] J.C. Schuster, M. Palm, Reassessment of the binary aluminum–titanium phase diagram, *J. Phase Equilibria Diffusion* 27 (2006) 255.
- [24] R.R. Zope, Y. Mishin, Interatomic potentials for atomistic simulations of the Ti–Al system, *Phys. Rev. B* 68 (2003) 241021.
- [25] R.E. Watson, M. Weinert, Transition-metal aluminide formation: Ti, V, Fe, and Ni aluminides, *Phys. Rev. B* 58 (1998) 5981.
- [26] J.L. Murray, Calculation of the titanium–aluminium phase diagram, *Metall. Trans. A* 19 (1988) 243.
- [27] I. Ansara, M. Dinsdale, M.H. Rand (Eds.), COST 507, Thermochemical Database for the Light Metal Alloys, vol. 2, European Communities, Luxembourg, 1998.
- [28] A.T. Dinsdale, SGTE data for pure elements, *Calphad* 15 (1991) 317.
- [29] I.I. Kornilov, E.N. Pylaeva, M.A. Volkova, P.I. Kripyakevich, V.Y. Markiv, Phase structure of alloys in the binary system Ti–Al containing from 0 to 30% Al, *Dokl. Akad. Nauk SSSR* 161 (1965) 843.
- [30] K. Ouchi, Y. Iijima, K. Hirano, Chapter. Interdiffusion in Ti–Al system, *Titanium '80, Science and Technology*, vol. 1, TMS, 1980, p. 559.
- [31] P.L. Martin, H.A. Lipsitt, N.T. Nuhfer, J.C. Williams, The effects of alloying on the microstructure and properties of Ti₃Al and TiAl, *Titanium '80, Science and Technology*, vol. 2, TMS, 1980, p. 1245.
- [32] E.W. Collings, Magnetic investigations of electronic bonding and α through γ phase equilibria in the titanium aluminum system, *Titanium and Titanium Alloys*, vol. 2, Plenum Press, 1982, p. 1391.
- [33] R.M. Waterstrat, Effect of Interstitial Elements on Phase Relationships in the Titanium–Aluminum System, NISTIR 88-3856, Technical Report, US Department of Commerce, 1988.
- [34] A. Suzuki, M. Takeyama, T. Matsuo, Transmission electron microscopy on the phase equilibria among β , α and α_2 phases in Ti–Al binary system, *Intermetallics* 10 (2002) 915.
- [35] E. Ence, H. Margolin, Phase relations in the titanium–aluminum system, *Trans. Metall. Soc. AIME* 221 (1961) 151.
- [36] P.A. Farrar, H. Margolin, Air Force Materials Laboratory Technology Report-65-69, Technical Report, Air Force Materials Laboratory, 1965.
- [37] L.A. Willey, H. Margolin, Al–Ti Aluminium–Titanium, *Metals Handbook*, 8th edition, ASM, Metals Park, OH, 1973, p. 264.
- [38] D. Clark, K.S. Jepson, G.I. Lewis, A study of the titanium–aluminium system up to 40 at.-% aluminum, *Jpn. Inst. Metals* 91 (1962/63) 197.
- [39] I.I. Kornilov, T.T. Nartova, S.P. Chernyshova, The Ti-rich range of the Ti–Al phase diagram, *Russ. Metall.* 6 (1976) 156.
- [40] T. Tsujimoto, M. Adachi, Reinvestigation of the Titanium-rich region of the titanium–aluminium equilibrium diagram, *Jpn. Inst. Metals* 94 (1966) 358.
- [41] T. Tsujimoto, M. Adachi, Study on the titanium-rich region of the titanium–aluminium equilibrium diagram, *Trans. Natl. Res. Inst. Metals* 9 (1976) 9.
- [42] H. Sasano, T. Tsujimoto, On the quenched structure and aging process of Ti–8–15.8 wt% Al alloy, *Titanium Science and Technology*, vol. 3, Plenum Press, New York, 1973, pp. 1635–1647.
- [43] R. Kainuma, M. Palm, G. Inden, Solid-phase equilibria in the Ti-rich part of the Ti–Al system, *Intermetallics* 2 (1994) 321.